www.czasopisma.pan.pl PAN www.journals.pan.pl
Opto-Electronics Review 25 (2017) 24–32

Contents lists available at ScienceDirect

Opto-Electronics Review

journal homepage: http://www.journals.elsevier.com/opto-electronics review

Improve a 3D distance measurement accuracy in stereo vision systems using optimization methods' approach

J.C. Rodríguez-Quiñonez[a,*], O. Sergiyenko[b], W. Flores-Fuentes[a], M. Rivas-lopez[b], D. Hernandez-Balbuena[a], R. Rascón[a], P. Mercorelli[c]

[a] Facultad de Ingeniería, Universidad Autónoma de Baja California, Blvd. Benito Juarez S/N, Mexicali, Baja California, CP 21280, Mexico
[b] Instituto de Ingeniería, Universidad Autónoma de Baja California, Normal S/N y Blvd. Benito Juárez, Mexicali, Baja California, CP 21280, Mexico
[c] Institute of Product and Process Information, Leuphana University of Lueneburg Volgershall 1, Lueneburg, Germany

ARTICLE INFO

Article history:
Available online 6 April 2017

Keywords:
Stereo vision
Optimization methods
Distance measurement

ABSTRACT

This paper presents a 3D distance measurement accuracy improvement for stereo vision systems using optimization methods A Stereo Vision system is developed and tested to identify common uncertainty sources. As the optimization methods are used to train a neural network, the resulting equation can be implemented in real time stereo vision systems. Computational experiments and a comparative analysis are conducted to identify a training function with a minimal error performance for such method. The offered method provides a general purpose modelling technique, attending diverse problems that affect stereo vision systems. Finally, the proposed method is applied in the developed stereo vision system and a statistical analysis is performed to validate the obtained improvements.

1. Introduction

A 3D measuring technique has many practical applications in material inspection, strain measurement, online monitoring, robot navigation, structural health monitoring, machinery processing, quality testing, depth information, object motion, etc. [1–5]. Stereo vision is a typical and widely used system in a 3D measurement. In this method two cameras, viewing from different angles, capture images [6]. Corner feature points are detected in these images of each stereo pairs [7]. These feature points are then triangulated at each frame based on stereo correspondences [7]. Using the stereo vision technique, 3D scanners can capture the three-dimensional shape of objects accurately or can be used to measure distances, angles or deformations. As technologies evolve, there have been high demands for 3D shape measurement techniques to possess the following combined technical features: high accuracy, fast speed and easy implementation [8]. However, to obtain these features in a single system is not always possible and the need to prioritize the systems' capabilities is required. Therefore, we create a system with the purpose of a measurement distance between two different patterns. The developed prototype is presented in Fig. 1. Due to the application of this system which is now oriented to a 3D distance measurement, we can focus on high speed patterns' recognition feature, and perform triangulation at real time processing, to use in distance measuring applications.

The presented paper shows the implementation of the intensity pattern match method to the stereo vision system for a measurement of distance in real time applications, afterward a calibration method is proposed to decrease the uncertainty of the system caused by common problems in stereo vision systems. Comparing different optimization methods, it looks to find an optimization method that with a neural network allows to perform improvement of the measurements.

2. Developed stereo vision system

Stereo vision is the process of extracting 3D information from multiple 2D views of a scene [9]. A block diagram of our developed stereo vision system can be observed in Fig. 2, the whole process can be divided into four main tasks: pattern match, conversion pixel to angle, triangulation and adjustment by trained neural network.

In order to calculate the x, y and z coordinates of any reflected point from an obstacle surface, we developed a set of equations derived from the law of sines [Eqs. (1)–(3)] [1].

$$x = a\frac{\sin C * \sin B}{\sin(B + C)}, \tag{1}$$

* Corresponding author.
E-mail address: julio.rodriguez81@uabc.edu.mx (J.C. Rodríguez-Quiñonez).

http://dx.doi.org/10.1016/j.opelre.2017.03.001
1230-3402/

Fig. 1. Developed stereo vision system with implemented control in LabVIEW.

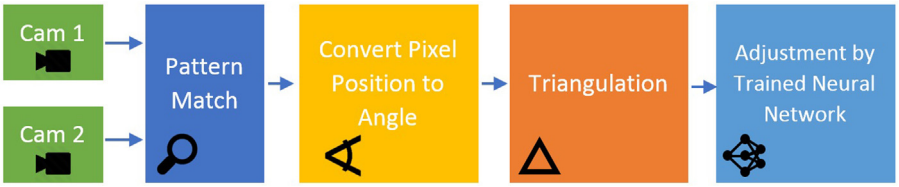

Fig. 2. Block diagram of developed stereo vision system.

$$y = a\left(\frac{1}{2} - \frac{\sin C * \cos B}{\sin(B+C)}\right), \tag{2}$$

$$z = a\left(\frac{\sin C * \sin B * \sin \beta}{\sin(B+C)}\right). \tag{3}$$

As seen in Fig. 3 these equations require the angles B, C, β and a fixed distance between the two cameras. The left and right cameras have the same specifications, the horizontal field of view (FOV) is of 66.22°, and the vertical FOV is of 40.66°. This results in a resolution of 0.034° per pixel in the horizontal plane and 0.037° per pixel in vertical plane.

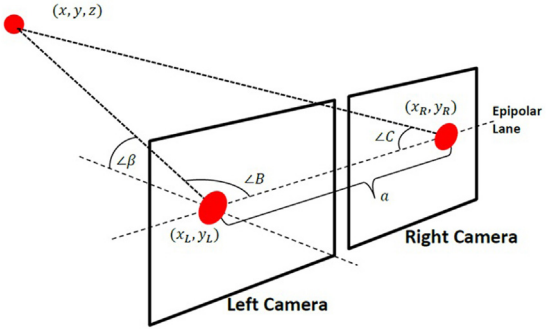

Fig. 3. Angles and coordinates obtained by the stereo vision system.

2.1. Stereo vision system description

The developed vision system uses two high definition cameras (1920 × 1080 px), with a frame rate of 30 fps, both cameras are separated by a distance of 50 cm and the main optical axis of the cameras are parallel to each other, the used vision model is the pin hole, therefore, were experimentally obtained the fields of view of each camera (vertical and horizontal) and the correspondence between each pixel-angle was calculated. For distance measurement applications, the system expects two different patterns (known in advance), if more than two similar patterns are detected, the system will use the patterns with the highest score, where the score relates how closely the template resembles the located matches (in a range of 0–1000). The unique constraint is if two or more arbitrary occurred patterns have exactly the same score, the system will consider the first detected pattern; but the probability of such event is minimal. In Fig. 3, we can see how the epipolar geometry approach was used to solve the correspondence problem, and how each of the angles is obtained and used to determine the spatial coordinates of the point of interest.

2.2. Intensity pattern match

The image match means that these images can be identified in the space or find a known image in another image, particularly, stereo matching is the field of study that aims to determine correspondences in two or more images shot from different viewpoints for obtaining a depth map of the actual scene [10]. It can recognize the unknown visual pattern by using the pattern that is stored in the computer, and build the relationship between the computer mode and the outer world. Pattern matching is the most common type of image match mode [11]. It is also called area-based image match. It uses correlation between brightness (intensity) patterns in the local neighbourhood of a pixel in one image and brightness patterns in the local neighbourhood in the other image, where the number of pairs of features to be considered becomes high [11].

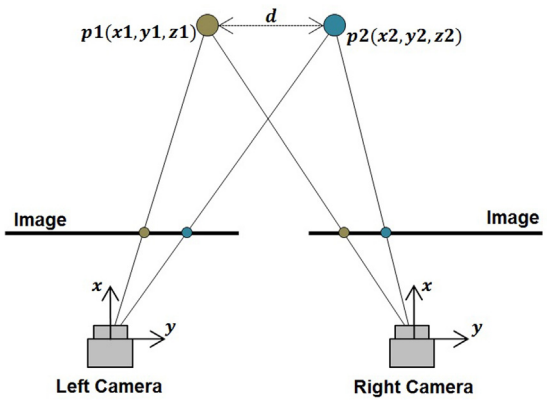

Fig. 4. Distance between two points of interest and their respective position in a stereo vision system.

2.3. *Application of stereo vision systems in measurement of distances and displacements*

One of the many applications of stereo vision systems is to measure distances and displacements. For a measurement displacement, our proposed stereo vision system is capable to follow two references in real time as in Fig. 4, making it possible to know the spatial coordinate of both references; then, by the formula of distance between two points $d = \sqrt{(x_2 - x_1)^2 + (y_2 - y_1)^2 + (z_2 - z_1)^2}$ it is possible to monitor the displacement in function of the time. Monitoring of displacements has multiple applications, among which are: geological monitoring, structural monitoring, stress analysis, occlusion detection, robot navigation, etc.

3. Calibration methods for stereo vision systems

Calibration methods of stereo vision systems are studied widely in the computer vision. The techniques found in literature for camera calibration can be in-situ (using the scene data of the camera and auxiliary data, as some 3D structures in the image area) or using calibration patterns [12]. In both cases the calibration can be broadly divided into three types: Linear methods, two step techniques and nonlinear methods [13–16]. Each with different constraints [15–21].

To improve the problems in the existing calibration constraints shown in Fig. 5 we develop train and implement neural networks with some selected parameters.

Neural networks have several meaningful features for a 3D measurement improvement in stereo vision systems. First, a network is made up of an interconnection of nonlinear neurons. Therefore, neural networks can learn the nonlinear imaging process [22,23]. Second, the basic idea behind supervised neural network learning and camera calibration are the same. The two use a set of data to find system parameters and then implement the parameters in data with the same characteristics, but not used during the training. Third, a neural network can provide a model-free solution for the problem (for some determined problems), which is in common with implicit camera calibration techniques [23]. Lastly, neural networks can be used in conjunction with typical calibration approaches. A post-processing of the system measurements (Previously calibrated by typical approaches, as shown in Fig. 5) can be performed using the trained neural network.

4. Artificial neural networks

An artificial neural network consists of computing units named neurons and connections between neurons named synapses. Synapses connect input neurons to hidden neurons and hidden

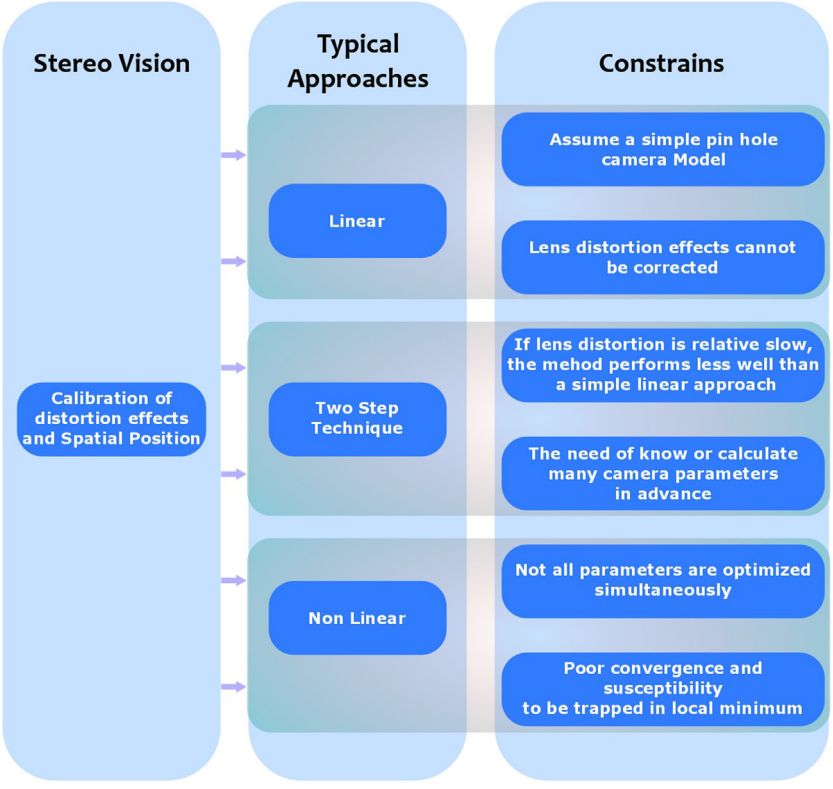

Fig. 5. Simplified diagram of typical calibrations and their constraints for stereo vision systems.

neurons to output neurons. The strength of the synapse from neuron i to neuron j is determined by means of a weight, W_{ij}. Input or independent variables are considered as neurons of an input layer, while dependent or output variables are considered as output neurons [24]. The nature of mapping relationship between input and output vectors is defined by these weights within the network. The input layer acts as an input data holder that distributes the input to the first hidden layer. The outputs from the first hidden layer then become the inputs to the second layer and so on. The last layer acts as the network output layer. In feedback network, signals propagate from output of any neuron to the input of any neuron [25]. The difference between predicted and target response produces an error signal which is used to modify the network weights. The adjustment of weights is intended to be in a direction that reduces the difference between network output and actual response vectors [25]. Due artificial neural networks are not restricted to linear correlations, they can be used for nonlinear applications [24]. There is no single best weight update function which can be applied for all nonlinear optimizations. The weight update function must be selected based on the characteristics of the problem. However, three different and commonly used weight update functions as: basic back propagation algorithm, conjugate gradient, and the Levenberg-Marquardt algorithm are discussed below. The three functions have been proved a good performance in the improvement of measurements in other 3D non-contact measurement technologies [26,27].

4.1. Back propagation algorithm

One common back propagation training algorithm is the gradient descendent. Gradient descendent moves the weights in a direction of the negative gradient to minimize the error function. A popular error performance function is the mean square error that is given by

$$MSE = \frac{1}{NP}\sum_{p=1}^{P}\sum_{j=1}^{N}(O_{pj} - t_{pj})^2, \tag{4}$$

where O_{pj} and t_{pj} are the actually predicted and target output values for example $p = 1, 2, P$ and output node $j = 1, 2, N$ [28]. Another popular error performance function is the mean absolute error that is given by

$$MAE = \frac{1}{T}\sum_{i=1}^{T}|(O_i - t_i)|, \tag{5}$$

where O_i, t_i and T are the predicted values, target values and total number of the test data, respectively [29,30].

Backpropagation calculate the derivative of the performance function with respect to the weight and bias variable matrix *(W)*. Each variable in W is adjusted according to the gradient descent algorithm with momentum and learning rate as follows

$$dW_t = m_c dW_{t-1} + l_r m_c \frac{d(PF)}{dW_t}, \tag{6}$$

where t is the number of epoch, W_{t-1} is the previous change to the weight or bias, lr is the learning rate, PF is the performance function, m_c is the momentum coefficient, and the performance objective function is assumed to be of quadratic form [25].

4.2. Nonlinear conjugate gradient techniques

Conjugate gradient type methods may be viewed as optimization techniques or as projection methods. Conjugate gradient type methods combine in an ideal fashion computational simplicity with certain optimality properties [31].

The basis for a nonlinear conjugate gradient method is to effectively apply the linear conjugate gradient method where the residual is replaced by the gradient. The first nonlinear conjugate gradient method was proposed by Fletcher and Reeves [32] as follows. Given the step direction p_k, use the line search to find the step length a_k such that $x_{k+1} = x_k + a_k p_k$. Then compute

$$\beta_{k+1} = \frac{\nabla f^T(x_{k+1}) \cdot \nabla f(x_{k+1})}{\nabla f^T(x_k) \cdot \nabla f(x_k)} \tag{7}$$

$$\beta_{k+1} = \beta_{k+1} p_k \nabla f(x_{k+1}). \tag{8}$$

Where β_{k+1} is the correction factor and is minimal in some cases. It is essential that the line search for choosing a_k satisfies the strong Wolfe conditions; this is necessary to ensure that the directions p_k are descent directions [32,26]. The advantage of conjugate gradient methods is that they need relatively little memory space for large-scale problems and require no numerical linear algebra, so each step is quite fast [26].

4.3. Levenberg-Marquardt method

Levenberg-Marquardt is a procedure used in the least squares fitting problem (as main application) [27,33,34]. The Levenberg algorithm can be expressed as

$$\left(\mathrm{J}^{\mathrm{T}}\mathrm{J}\right)\delta = \mathrm{J}^{\mathrm{T}}\left[\mathrm{y} - \mathrm{f}\left(\beta\right)\right], \tag{9}$$

where $\boldsymbol{J}$ is the Jacobian matrix [35] whose i^{th} row equals J_i, and where $\boldsymbol{f}$ and $\boldsymbol{y}$ are the vectors with i^{th} component $f(xi; \beta)$ and y_i, respectively. This is a set of linear equations which can be solved for $\boldsymbol{\delta}$.

Marquardt's contribution [26] is to replace this equation by a damped version

$$\left(\mathrm{J}^{\mathrm{T}}\mathrm{J} + \lambda\mathrm{I}\right)\delta = \mathrm{J}^{\mathrm{T}}\left[\mathrm{y} - \mathrm{f}(\beta)\right], \tag{10}$$

and to avoid slow convergence Marquardt [36] replaced the identity matrix, $\boldsymbol{I}$, with the diagonal of $\boldsymbol{J^TJ}$, resulting in the Levenberg-Marquardt algorithm

$$(\mathrm{J}^{\mathrm{T}}\mathrm{J} + \lambda diag(\mathrm{J}^{\mathrm{T}}\mathrm{J}))\delta = \mathrm{J}^{\mathrm{T}}[\mathrm{y} - \mathrm{f}(\beta)]. \tag{11}$$

5. Experimentation results and statistical analysis of the obtained data

To improve the 3D measurement accuracy, special routines have been developed in Matlab and LabVIEW, enabling to test with different training patters, training functions, learning functions and learning rates. A program has been developed in LabVIEW to stereo view a pattern with known distance measures, and to allow us to change multiple parameters, as: camera Field of View (FOV) for different cameras, distance between cameras, learning rate, error function, learning function, and Weight bias learning function. The used pattern can be changed in size, number of rows and columns and these parameters can be adjusted in our developed software. To improve the 3D distance measurement accuracy in the developed stereo vision system, the distance among several points of the given pattern is obtained and used to train a neural network, the input data are a matrix of the calculated coordinates x_1, y_1, z_1, x_2, y_2, z_2 and the real distance among each pair of points. The neural network have four hyperbolic tangent sigmoid transfer functions as inputs hidden layers and one linear transfer function as an output layer, the target is the real distance among each point. The training functions and learning rates were experimentally modified to obtain the best adjustment of measurements. The measurements used to train the neural network are: 207 distance measurement samples from the calibration pattern; 155 measurement samples as training data of the neural network,

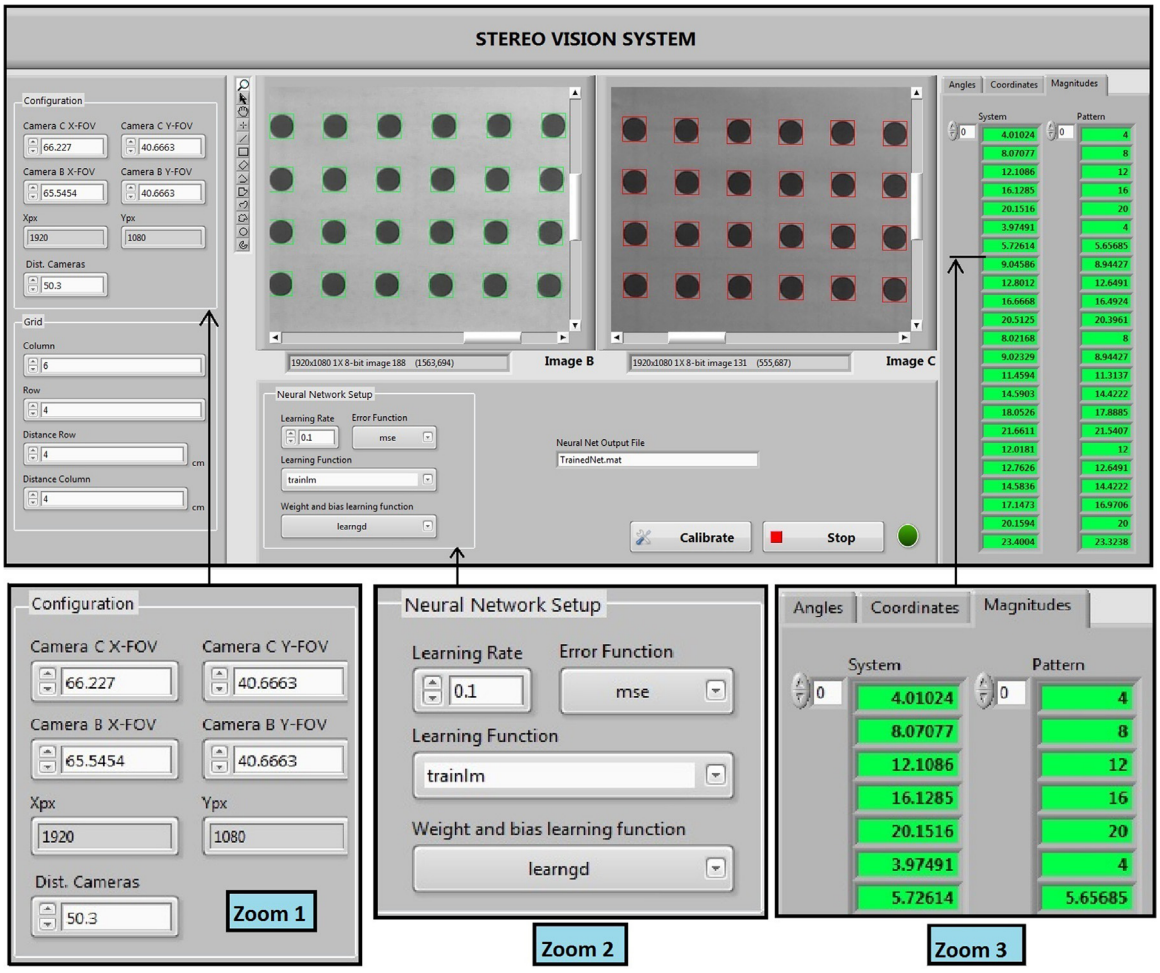

Fig. 6. Stereo view of our developed system, the magnitudes on the right side *(green)* correspond to the real magnitudes of the pattern and calculated by the system before the measurement improvement.

26 measurement samples as test data and 26 measurement samples as validation. To improve the distance measurement accuracy, the trained neural network calculates a function that compensates measurement errors of the system and determine the actual distance between samples, this allows to directly adjust the distance measurements between objects of interest and removes the uncertainty related to the spatial position of the system against the object of interest. The developed software in LabVIEW is presented in Fig. 6.

The proposed method was implemented in LabVIEW and Matlab. LabVIEW was used for image analysis, specifically for the pattern match and coordinate localization of the objects of interest. The calculation of the coordinates and the triangulation equations was implemented in LabVIEW, while the measurement data (the spatial coordinate and the distance of each interest object) of the pinhole model were exported to Matlab to perform the neural network training and proper validation. Table 1 shows the analysis summary of the system (the measured coordinates, calculated distance and real distance) and the error of each measurement before improving the distance measurement accuracy. The standard deviation of the error in the system is of 0.1115 cm (without the proposed method).

Three known techniques were compared and used to train neural networks: resilient backpropagation, scaled conjugate gradient, and Levenberg-Marquardt. This was performed to select the training function that achieves a better adjustment of the measurements in the proposed vision system. For comparison, the average performance of each technique is calculated at different learning rates, the training function with better performance is selected, and for this application the Levenberg-Marquardt function shows a better average performance as in Fig. 7.

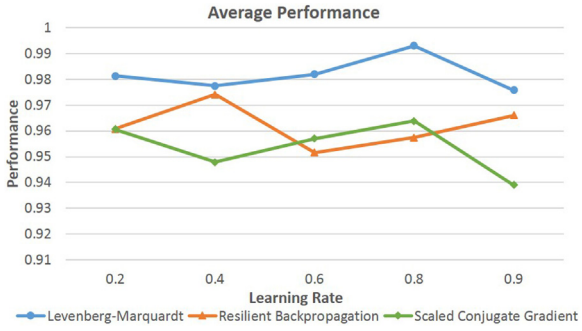

Fig. 7. Comparing the performance of three weight update functions at different learning rates.

As mentioned before, the backpropagation training function is Levenberg-Marquardt and the network weights are modified so that the error between the actual output and desired output is reduced. Since it is difficult to analytically calculate the learning rate to which a neural network will have a better performance, we decided to test each method on five different learning rates, with a result of 0.8 for the best performance (as seen in Fig. 7). The learning function for the weight and bias is the conjugate gradient

Table 1
Stereo Vision System measurements and distance calculation (Simplified table).

Measured Coordinates (cm)						Distance		Absolute Error (cm)
x_1	y_1	z_1	x_2	y_2	z_2	Calculated	Real	d
80.1546	*11.013*	*0.368734*	*81.754*	*4.39364*	*0.21491*	15.4902	15.2	0.2902
80.1546	*11.013*	*0.368734*	*81.8007*	*3.35638*	*7.30139*	10.9619	10.748	0.2139
81.754	*4.39364*	*3.59859*	*81.0188*	*8.17828*	*7.28463*	5.33395	5.37401	0.04006
81.902	*0.693892*	*4.03523*	*81.7407*	*4.55411*	*3.97363*	3.86408	3.8	0.06408
80.2753	*10.893*	*4.11315*	*81.8007*	*3.35638*	*0.268791*	8.59693	8.49706	0.09987
81.9015	*0.532848*	*3.5513*	*81.9888*	*0.506594*	*7.31819*	3.76799	3.8	0.03201
81.7407	*4.55411*	*3.97363*	*80.1546*	*11.013*	*0.368734*	16.0575	15.6678	0.3897
81.7407	*4.55411*	*3.97363*	*81.1009*	*8.21204*	*0.159895*	5.323	5.37401	0.05101

Table 2
Stereo Vision System measurements, adjusted distance and calculated error (Simplified table).

Measured Coordinates (cm)						Distance		Absolute Error (cm)
x_1	y_1	z_1	x_2	y_2	z_2	Adjusted by the neural network	Real	d
80.1546	11.013	0.368734	81.754	4.39364	0.21491	15.1526	15.2	0.04739
80.1546	11.013	0.368734	81.8007	3.35638	7.30139	10.8398	10.748	0.09188
81.754	4.39364	3.59859	81.0188	8.17828	7.28463	5.33384	5.37401	0.04016
81.902	0.693892	4.03523	81.7407	4.55411	3.97363	3.80811	3.8	0.00811
80.2753	10.893	4.11315	81.8007	3.35638	0.268791	8.45094	8.49706	0.04611
81.9015	0.532848	3.5513	81.9888	0.506594	7.31819	3.74325	3.8	0.05674
81.7407	4.55411	3.97363	80.1546	11.013	0.368734	15.6594	15.6678	0.00834
81.7407	4.55411	3.97363	81.1009	8.21204	0.159895	5.32619	5.37401	0.04781

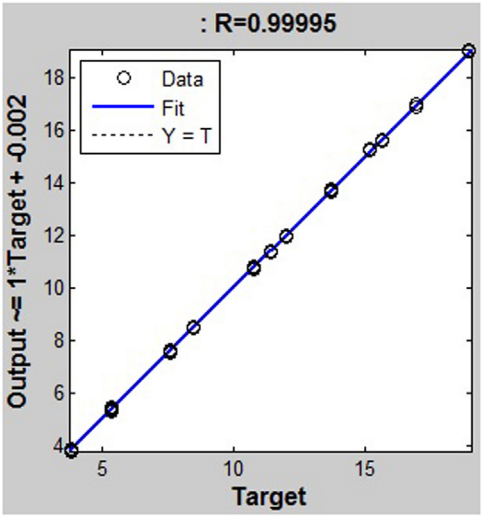

Fig. 8. Regression analysis of the adjustment.

and the function error is a mean square error. The neural network was trained until the result of a conducted regression provides an R > 0.999 as in Fig. 8.

Therefore, after all previous considerations, the proposed neural network was created as follows: 3 hidden layers with 5 neurons per layer, each layer with the hyperbolic tangent sigmoid transfer function, the backpropagation training function was Levenberg-Marquardt, the learning rate was of 0.8, the learning function for the weight and bias is the conjugate gradient and the function error is a mean square error. After the neural network training, a comparison between the system with and without the neural network was performed, we tested 69 distance measurements (independent from the previous 207 measurements) using the proposed stereo vision system. A direct comparison between both measurements, with and without the proposed improvement can be observed on the zoom images of Fig. 9, as can be appreciated, the measurements in the Zoom2 are fit with the real values, otherwise Zoom1 measurements have a dephasing in respect to the real values. In Fig. 9(a), the measurements only approximate to the real value, but still have an average uncertainty of 0.1249 cm. The result after improving the measurements by the proposed method and applying the adjustment of measurements is shown in Fig. 9(b), the average measurement uncertainty after the calibration is of 0.0254 cm, 79.66% better than the original measurement uncertainty.

Therefore, a summary of the experimentation is presented in Table 2, the main difference with Table 1 is the distance adjusted by the neural network which presents a standard deviation of error after the calibration of 0.03258 cm.

The proposed calibration was performed in other two scenarios, first by varying the angular position of the system with respect to the calibration pattern in 20° and, second, by varying the angular position of the system with respect to the calibration pattern in 30° (Tables 3 and 4, respectively).

After the proposed improvement, in the first scenario where a variation of the angular position of the system with respect the calibration pattern is 20° the obtained standard deviation is of 0.05273 cm and in the second scenario where a variation of the angular position of the system with respect the calibration pattern is 30° the obtained standard deviation is of 0.04994 cm. As can be observed the differences on the standard deviation between a 20° and 30° variations is minimal, however, when this standard deviation is compared with the standard deviation of the system without angular position variations, a difference can be perceived, this is due to the angular position variation of the system and the increment of the distance between the calibration pattern and the system (as can be seen on coordinates x_1 and x_2 of Tables 2–4).

Additional to the regression, a residual analysis was performed. In Fig. 10 two residual plots can be seen. The first plot is the residual analysis between the real distance and the measured distance without the proposed adjustment, the second plot is the residual analysis between the real distance and the measured distance after the adjustment using the proposed neural network. Both residual plots corresponded to the same distance measurements, as can be observed in Fig. 10 the distance measurement of our proposed

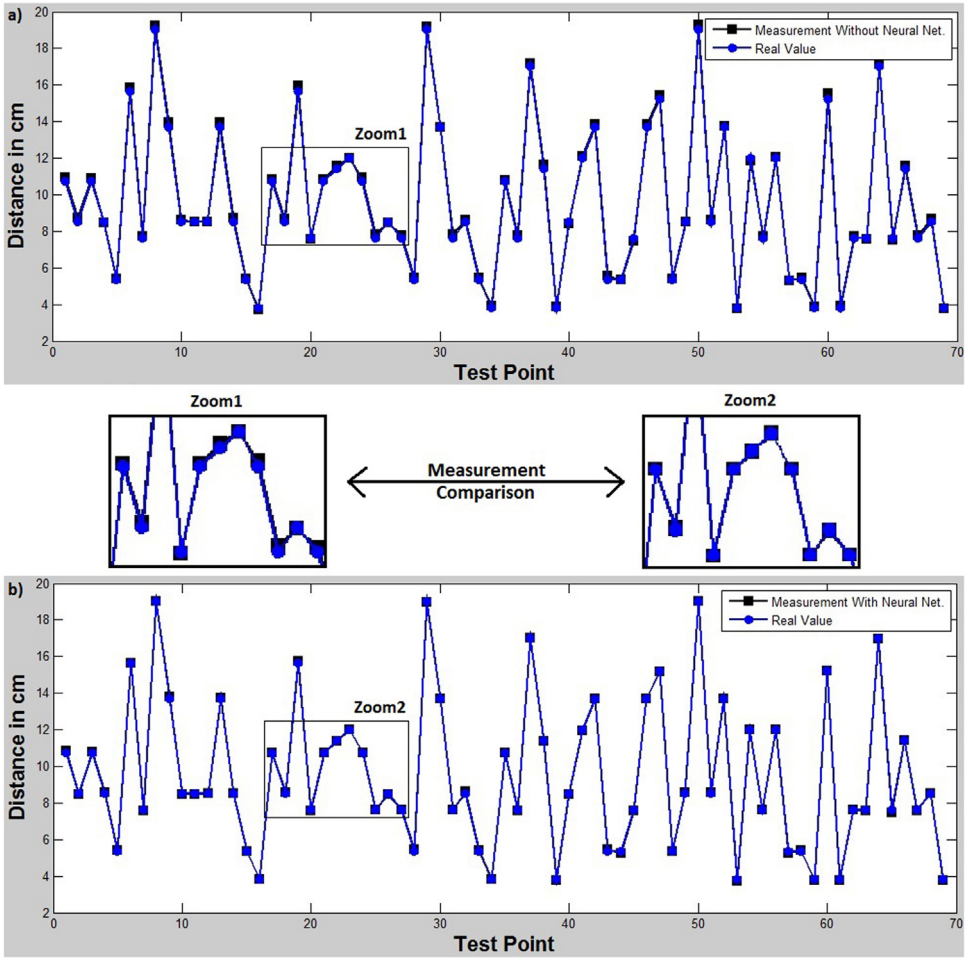

Fig. 9. Comparing the measurements performed by the system with and without the proposed improvement *vs*. the real distances, a) measurements without the adjustment by the obtained function trained by the neural network, b) measurements after adjustment with the function trained by the neural network.

Table 4
Stereo Vision System measurements, adjusted distance and calculated error with angular position variation of the system in 30° (Simplified table).

Measured Coordinates (cm)						Distance		Absolute Error (cm)
x_1	y_1	z_1	x_2	y_2	z_2	Adjusted by the neural network	Real	d
109.984	13.7728	8.73664	108.996	9.98659	4.51146	5.65298	5.65685	0.00386
109.984	13.7728	8.73664	108.812	10.1443	−4.2894	12.6465	12.6491	0.00251
108.853	9.9404	8.86074	107.539	6.11704	0.14134	8.91435	8.94427	0.02991
107.548	6.04939	8.89537	105.899	2.21211	−4.2442	12.6895	12.6491	0.04049
106.043	2.1811	4.52846	108.826	10.0764	0.14303	8.89444	8.94427	0.04982
107.539	6.11704	0.14134	101.727	−5.6877	0.20056	12.0200	12.000	0.02021
108.826	10.0764	0.14303	109.947	13.909	−4.26203	5.58594	5.65685	0.07090
109.947	13.909	−4.26203	105.899	2.21215	−4.2442	11.9600	12.000	0.03995

Table 3
Stereo Vision System measurements, adjusted distance and calculated error with angular position variation of the system in 20° (Simplified table).

Measured Coordinates (cm)						Distance		Absolute Error (cm)
x_1	y_1	z_1	x_2	y_2	z_2	Adjusted by the neural network	Real	d
107.589	17.0577	8.54641	106.884	13.256	8.63043	3.96861	4.00	0.03138
107.589	17.0577	8.54641	103.185	1.44462	4.40644	16.4754	16.4924	0.01697
106.884	13.256	8.63043	105.997	9.37236	8.6977	3.97419	4.00	0.02580
105.997	9.37236	8.6977	107.567	17.1238	4.24039	8.86078	8.94427	0.08348
103.379	2.5076	8.71707	104.756	5.51324	4.40474	14.3922	14.4222	0.02998
107.021	13.3053	4.28915	107.523	17.2559	−4.37986	8.94194	8.94427	0.00239
104.907	5.42028	4.34219	105.823	9.82716	−4.38011	8.96849	8.94427	0.02422
106.849	13.3888	−0.0702	104.756	5.51324	−4.40474	8.93042	8.94427	0.01384

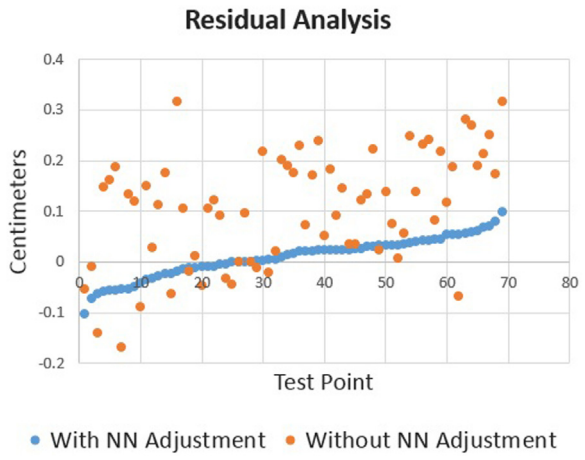

Fig. 10. Residual analysis of the system with and without the proposed measurement adjustment.

system has a variability between −1.0 mm to 1.0 mm while the system without adjustment has a variability between −1.7 mm and 3.2 mm.

The proposed method provides an improved accuracy in measuring distances on stereo vision systems. This method has been tested in our system, however, does not depend on any physical variable of our system, the method has the capability to be used in any other stereo vision system. In addition to offering the improved accuracy, this technique incorporating neural networks offers benefits associated with a general purpose modelling technique, attending the diverse problems that affect stereo vision systems which in some cases are independent of each other. Therefore, as well as providing correction of radial lens distortion, the network can allow for nonlinear errors caused by factors such as misalignment of the CCD with the camera body, non-axial mounting of CCD and lens, focal length, the image coordinate centre, and manufacturing errors in the lens and CCD [17].

6. Conclusions

Comparing between three different optimization methods the Levenberg-Marquardt method provides better performance than resilent backpropagation and scaled conjugate gradient. The result is a neural network that shows reliability in a distance measurement improvement of stereo vision systems. As the final result of a neural network is a mathematical function, the adjustment of a distance measurement can be realized in 12 ms, this execution time was obtained using a computer with an Intel Core i7-4710MQ CPU 2.50 GHz. To corroborate the improvements, experimental measurements where performed. Measuring from a distance of 0.8 meter, results in a standard deviation of the system of 0.03258 cm, and from a distance of 1.0 meter with angular position variation of the calibration pattern in 30° and 20° the standard deviation of the system is of 0.04994 cm and 0.05273 cm, respectively. Therefore, the measurement improvement of the system is 79.66% better then the use only of a pin hole model, the residual analysis in Fig. 10 has shown a decreased error of the measurements with a variability between −1.0 mm to 1.0 mm while the system without adjustment has a variability between −1.7 mm and 3.2 mm. The proposed method can be used to calibrate stereo vision systems that require reliable distance measurements for decision making or capture information in real time, that combine two main tasks. First, the object tracking on real time (limited by the fps of the camera) by intensity pattern match localization methods, and second the distance measurement and adjustment on real time, faster than the camera refresh (once trained a neural network, the resulting net has to process simple math calculations and adjust the measurements). The techniques presented are considered to offer improved distance measurements for multiple machine vision applications, particularly machine vision applications in dynamic environments, measuring coordinates and distances in real time.

Acknowledgements

This work was supported partially by the Autonomous University of Baja California, Campus Mexicali, Blvd. Benito Juarez s/n C.P. 21280, Mexicali, Baja California, Mexico, with the project 105/6/N/13/1, and by PRODEP 2014-2015.

References

[1] L.C. Básaca-Preciado, O.Y. Sergiyenko, J.C. Rodríguez-Quinonez, X. García, V.V. Tyrsa, M. Rivas-Lopez, D. Hernandez-Balbuena, P. Mercorelli, M. Podrygalo, A. Gurko, I. Tabakova, O. Starostenko, Optical 3D laser measurement system for navigation of autonomous mobile robot, Opt. Laser Eng. 54 (2014) 159–169, http://dx.doi.org/10.1016/j.optlaseng.2013.08.005.
[2] W. Flores-Fuentes, M. Rivas-Lopez, O. Sergiyenko, J. Rodriguez-Quinonez, D. Hernandez-Balbuena, J. Rivera-Castillo, Energy centre detection in light scanning sensors for structural health monitoring accuracy enhancement, IEEE J. Sens. 14 (2014) 2355–2361, http://dx.doi.org/10.1109/JSEN.2014.2310224.
[3] J.C. Rodríguez-Quiñonez, O.Y. Sergiyenko, L.C.B. Preciado, V.V. Tyrsa, A.G. Gurko, M.A. Podrygalo, M.R. Lopez, D.H. Balbuena, Optical monitoring of scoliosis by 3D medical laser scanner, Opt. Laser Eng. 54 (2014) 175–186, http://dx.doi.org/10.1016/j.optlaseng.2013.07.026.
[4] F. Huang, K.-K. Fehrs, G. Hartmann, R. Klette, Wide-angle vision for road views, Opto-Electron. Rev. 21 (2013) 1–22.
[5] T. Hachaj, M. Ogiela, Real time area-based stereo matching algorithm for multimedia video devices, Opto-Electron. Rev. 21 (2013) 367–375.
[6] H. Zhao, Z. Wang, H. Jiang, Y. Xu, C. Dong, Calibration for stereo vision system based on phase matching and bundle adjustment algorithm, Opt. Laser Eng. 68 (2015) 203–213.
[7] J. Xue, X. Su, A new approach for the bundle adjustment problem with fixed constraints in stereo vision, Optik –Int. J. Light Electron Opt. 123 (2012) 1923–1927, http://dx.doi.org/10.1016/j.ijleo.2011.09.025.
[8] Z. Wang, D.A. Nguyen, J. Barnes, Recent advances in 3D shape measurement and imaging using fringe projection technique, in: SEM Annual Congress and Exposition on Experimental and Applied Mechanics, Albuquerque, New Mexico, 2009.
[9] G. Saygili, L. van der Maaten, E.A. Hendriks, Adaptive stereo similarity fusion using confidence measures, Comput. Vis. Image Und. 135 (2015) 95–108, http://dx.doi.org/10.1016/j.cviu.2015.02.005.
[10] S. Ploumpis, A. Amanatiadis, A. Gasteratos, A stereo matching approach based on particle filters and scattered control landmarks, Image Vision Comput. (2015), http://dx.doi.org/10.1016/j.imavis.2015.04.001.
[11] Z. Zhu, T. Lin, Y. Piao, S. Chen, Recognition of the initial position of weld based on the image pattern match technology for welding robot, Int. J. Adv. Manuf. Tech. 26 (2005) 784–788, http://dx.doi.org/10.1007/s00170-003-2053-8.
[12] R. Galego, A. Ortega, R. Ferreira, A. Bernardino, J. Andrade Cetto, J. Gaspar, Uncertainty analysis of the dlt-lines calibration algorithm for cameras with radial distortion, Comput. Vis. Image Und. 140 (2015) 115–126.
[13] J. Salvi, X. Armangu_e, J. Batlle, A comparative review of camera calibrating methods with accuracy evaluation, Pattern recogn. 35 (2002) 1617–1635.
[14] D. Garcia, J.-J. Orteu, M. Devy, Accurate calibration of a stereovision sensor: Comparison of different approaches, VMV (2000) 25–32.
[15] L. Mei-Song, M. Ping-Wang, L. Lu, H. Jing-Huan, High precision camera calibration in vision measurement, Opt. Laser Tech. 39 (2007) 1413–1420.
[16] S. Sheng-Wen, H. Yi-Ping, L. Wei-Song, Accurate linear technique for camera calibration considering lens distortion by solving an eigenvalue problem, Opt. Eng. 32 (1993) 138–149.
[17] L.N. Smith, M.L. Smith, Automatic machine vision calibration using statistical and neural network methods, Image Vis. Comput. 23 (2005) 887–899.
[18] R. Klette, A. Koschan, K. Schluns, Computer Vision: Three Dimensional Data from Images, Springer, 1998.
[19] S. Chao-Ton, C.A. Chang, T. Fang-Chih, Neural networks for precise measurement in computer vision systems, Comput. Ind. 27 (1995) 5–236.
[20] Q. Memon, S. Khan, Camera calibration and three-dimensional world reconstruction of stereo-vision using neural networks, Int. J. Syst. Sci. 32 (2001) 1155–1159.
[21] C. Zhou, Y. Du, Y. Tang, A high-precision calibration method for stereo vision system, in: A. Bhatti (Ed.), Advances in Theory and Applications of Stereo Vision, InTech, 2011, 2017.
[22] M.B. Lynch, C.H. Dagli, M. Vallenki, The use of feedforward neural networks for machine vision calibration, Int. J. Prod. Econ. 60–61 (1999) 479–489.
[23] Y. Do, Application of neural networks for stereo-camera calibration, Neural Networks IEEE Int. Joint Conf. 4 (1999) 2719–2722.

[24] M. Jalali-Heravi, M. Asadollahi-Baboli, P. Shahbazikhah, Qsar study of heparanase inhibitors activity using artificial neural networks and levenberg-marquardt algorithm, Eur. J. Med. Chem. 43 (2008) 548–556.
[25] I. Mukherjee, S. Routroy, Comparing the performance of neural networks developed by using levenberg-marquardt and quasi-newton with the gradient descent algorithm for modelling a multiple response grinding process, Expert Syst. Appl. 39 (2012) 2397–2407.
[26] J.C. Rodriguez-Quinonez, O. Sergiyenko, F.F. Gonzalez-Navarro, L. Basaca-Preciado, V. Tyrsa, Surface recognition improvement in 3D medical laser scanner using levenberg-marquardt method, Signal Process 93 (2013) 378–386.
[27] J. Rodríguez-Quiñonez, O. Sergiyenko, D. Hernandez-Balbuena, M. Rivas-Lopez, W. Flores-Fuentes, L. Basaca-Preciado, Improve 3D laser scanner measurements accuracy using a ffbp neural network with widrow-hoff weight/bias learning function, Opto-Electron. Rev. 22 (2014) 224–235.
[28] R.S. Sexton, J.N. Gupta, Comparative evaluation of genetic algorithm and backpropagation for training neural networks, Inf. Sci. 129 (2000) 5–59.
[29] M. Hayati, Z. Mohebi, Application of artificial neural networks for temperature forecasting World Academy of Science, Eng. Technol. 28 (2007) 275–279.
[30] E. Guresen, G. Kayakutlu, T.U. Daim, Using artificial neural network models in stock market index prediction, Expert Syst. Appl. 38 (2011) 10389–10397.
[31] M. Hanke, Conjugate gradient type methods for ill-posed problems, Vol. 327, CRC Press, 1995, 2017, pp. 327.
[32] J. Nocedal, S.J. Wright, Numerical Optimization, Springer, 1999.
[33] A. Abba, F. Caponio, A. Geraci, G. Ripamontii, Non-linear least-squares in fpga devices for digital spectroscopy, Nuclear Science Symp. Conf. Record (2009) 563–568, Orlando.
[34] C. Herold, V. Despiegel, S. Gentric, S. Dubuisson, I. Bloch, Recursive head reconstruction from multi-view video sequences, Comput. Vis. Image Und. 122 (2014) 182–201.
[35] B.M. Wilamowski, H. Yu, Improved computation for Levenberg-Marquardt training, IEEE Trans. Neural Netw. 21 (2010) 930–937.
[36] D. Marquardt, An algorithm for least-squares estimation of nonlinear parameters, SIAM J. Appl. Math. 11 (1963) 431–441.